frontiers | Frontiers in Earth Science

TYPE Original Research
PUBLISHED 12 August 2022
DOI 10.3389/feart.2022.946972

OPEN ACCESS

EDITED BY
Daoyang Yuan,
Lanzhou University, China

REVIEWED BY
Zhanyu Wei,
China Earthquake Administration, China
Junling Pei,
Chinese Academy of Geological Sciences (CAGS), China

*CORRESPONDENCE
Yigang Li,
liyig@263.net

SPECIALTY SECTION
This article was submitted to Structural Geology and Tectonics, a section of the journal Frontiers in Earth Science

RECEIVED 18 May 2022
ACCEPTED 08 July 2022
PUBLISHED 12 August 2022

CITATION
Liu K, Li Y, Nan Y, Liu B and Wang W (2022), Detailed shallow structure of the seismogenic fault of the 1976 M_S7.8 Tangshan earthquake, China.
Front. Earth Sci. 10:946972.
doi: 10.3389/feart.2022.946972

Detailed shallow structure of the seismogenic fault of the 1976 M_S7.8 Tangshan earthquake, China

Kang Liu[1,2], Yigang Li[1]*, Yanyun Nan[1], Baojin Liu[3] and Wanhe Wang[4]

[1]National Earthquake Response Support Service, Beijing, China, [2]Hebei Key Laboratory of Earthquake Dynamics, Institute of Disaster Prevention, Sanhe, China, [3]Geophysical Exploration Center, China Earthquake Administration, Zhengzhou, China, [4]Xi'an Research Institute Co., Ltd., China Coal Technology and Engineering Group Corp, Xi'an, China

In 1976, an M_S7.8 strong earthquake occurred in the Tangshan region of Northeast China within an ancient craton. In this study, we conducted shallow seismic exploration, drilling-based exploration, and exploratory trench excavation of ground fissures in the Tangshan Fault Zone and obtained a high-resolution shallow seismic profile. Through analysis of its lithology and sedimentary cycle, we constructed a composite drilling profile across the faults. Coupled with the shallow fault combination patterns identified from the exploratory trenches, the profile reveals that the Guye-Nanhu Fault was the shallow response fault in the seismogenic structure of the Tangshan earthquake. This fault is a strike-slip fault with a positive flower structure; the reverse fault branches become progressively steeper with depth and converge downward toward the vertical main strike-slip fault. A high-angle thrust fault is located to the west of the main strike-slip fault, and a series of small-scale normal faults appear in front of this fault, owing to local extension. The tectonic form revealed by the deep seismic reflection profiles further supports the superficial tectonic model. The near-NEE orientation of the stress field in North China and the lower strike-slip movement component of the Tanlu Fault Zone facilitate faulting in the Tangshan–Hejian–Xingtai Fault Zone, which lies diagonally in the middle rectangular area of the North China Plain faulted basin. The detailed structural model of the seismogenic fault obtained by various detection methods is of great significance for understanding the seismogenic mechanism of the Tangshan earthquake.

KEYWORDS

Tangshan earthquake, shallow seismic exploration, composite drilling profile, exploratory trench, deep seismic reflection profile, flower structure

Introduction

On 28 July 1976, an M_s7.8 strong earthquake struck Tangshan city in the North China Plain region, killing 242,000 people and destroying the entire city. As this high-magnitude earthquake occurred in the North China craton, its seismogenic structure has attracted substantial research attention.

For example, by investigating the homogenous distribution of fissures resulting from the Tangshan earthquake, it was initially proposed that the seismogenic fault was located in the Tangshan Fault Zone and corresponded to the NW-trending No. 5 seam of the Tangshan Mine, with a dip angle of 70–80° (Wang et al., 1981). However, the results of shallow artificial seismic exploration indicated that the seismogenic fault was an NW-trending, high-dip, right-lateral strike-slip fault with a normal component, causing dislocation of the Holocene and Pleistocene strata (Hao and You, 2001). Conversely, it has been suggested that the seismogenic fault is a high-angle, west-dipping, thrust fault with a strike-slip component and an offset of 15 m that accrued during the Late Pleistocene (You et al., 2002). Furthermore, in a study of ground subsidence in a strong earthquake area, Qiu et al. (2005) discovered a large fault related to the Tangshan earthquake called the Fuzhuang-Xihe Fault, with a length of approximately 90 km and an offset of 3 m at the surface, characterized as a shovel-shaped normal fault.

In recent years, shallow artificial seismic exploration, drilling-based exploration, and exploratory trench excavation conducted near the remains of Niumaku and Tangshan Asylum have revealed that the Tangshan Fault Zone exhibits features of reverse and strike-slip movements at shallow depths (Liu, 2011). A composite drilling columnar profile at the earthquake relic site of Tangshan No. 10 Middle School revealed a near-vertical fault beneath the surface cracks, with a dip angle >83° and a middle Pleistocene vertical throw of 40 m (Liu et al., 2013). Moreover, Guo et al. (2011) analyzed a composite drilling profile and an exploratory trench in Sunjialou, Tangshan, and proposed that the seismogenic fault of the Tangshan earthquake was a normal fault (Guo et al., 2011, Guo et al., 2017; Guo and Zhao, 2019).

After the earthquake, numerous studies employed deep detection methods in the Tangshan earthquake area, from which crustal models and crustal thickness distributions were acquired (Zeng et al., 1985; Zhang et al., 1994). For example, a low-velocity layer was discovered in the lower part of the Tangshan fault block, which rapidly pinches out on both sides (Long and Zelt, 1991; Zhang et al., 1994; Lai et al., 1998; An et al., 2009). The epicenter of the main shock was located at the intersection of the NE-trending low-velocity belt and the NW-trending high-velocity belt (Lai et al., 1998). Moreover, Shao et al. (1986) proposed that the Tangshan earthquake was located in the transition zone of upper mantle differential movement. Huang and Zhao (2006) obtained a 3D crustal P-wave velocity structure model of the Beijing–Tianjin–Tangshan area using accurate P-wave arrival time data from the dense digital seismic network of the capital region and found that high-conductivity and low-velocity anomalies under the Tangshan earthquake source area were related to the existence of fluids. Furthermore, according to data from a mobile seismic observation array and the receiver function inversion method, Liu et al. (2007) found that the crust–mantle interface in the Tangshan region has experienced clear fault-block uplift. Additionally, a 2D deep seismic reflection profile revealed the existence of a large flower structure system in the deep part of the Tangshan Fault Zone (Liu, 2011; Liu et al., 2011).

Li et al. (2017) argued that the presence of low-velocity bodies in the crust makes it easy for tectonic stresses to accumulate and thus trigger large earthquakes. Applying high-resolution seismic imaging of P and S waves, Li et al. (2018) proposed that the migration of magma from the mantle to the lower crust may be an important factor controlling strong earthquakes within the North China craton. In recent years, experimental work in dense urban areas using the horizontal-to-vertical spectral ratio (HVSR) method with a dense seismic array as a low-cost and effective survey method has revealed that the Tangshan Fault Zone has been damaged and modified by strong seismic activity since the Quaternary (Bao et al., 2018, Bao et al., 2019, 2021). Mearns and Sornette (2021) proposed "a transfer fault complex" to explain the dynamics and faulting mechanisms of the Tangshan earthquake. In this study, shallow seismic exploration, composite drilling profile, and exploratory trenches have been used to investigate the surface rupture zone of the 1976 Tangshan earthquake. Furthermore, the detailed structural form of the shallow structure of the seismogenic fault has been obtained to better understand the seismogenic structure of the Tangshan earthquake.

Geological background

The research area is located at the boundary region of two geological units: the Yanshan uplift and the North China Plain faulted basin. Since the Mesozoic and Cenozoic, the Yanshan Mountains have been rising continuously, whereas the Bohai Bay Basin has experienced strong subsidence (Guo et al., 1977). The research area has been in a state of tectonic uplift for a long time, with Paleogene and Neogene strata now missing from the stratigraphic record (Figure 1). During the Quaternary period, the crust differentiated from north to south, and rivers became widespread. Except for a few hills with exposed bedrock scattered in the northeastern mountainous area and Tangshan city, most of the region is covered by Quaternary alluvial deposits. Regional strata and drilling profile data show that the sediments are predominantly sandy clay and sandy gravel, with highly variable thickness, which are controlled by paleogeographic evolution. Generally, the thickness of the Quaternary deposits

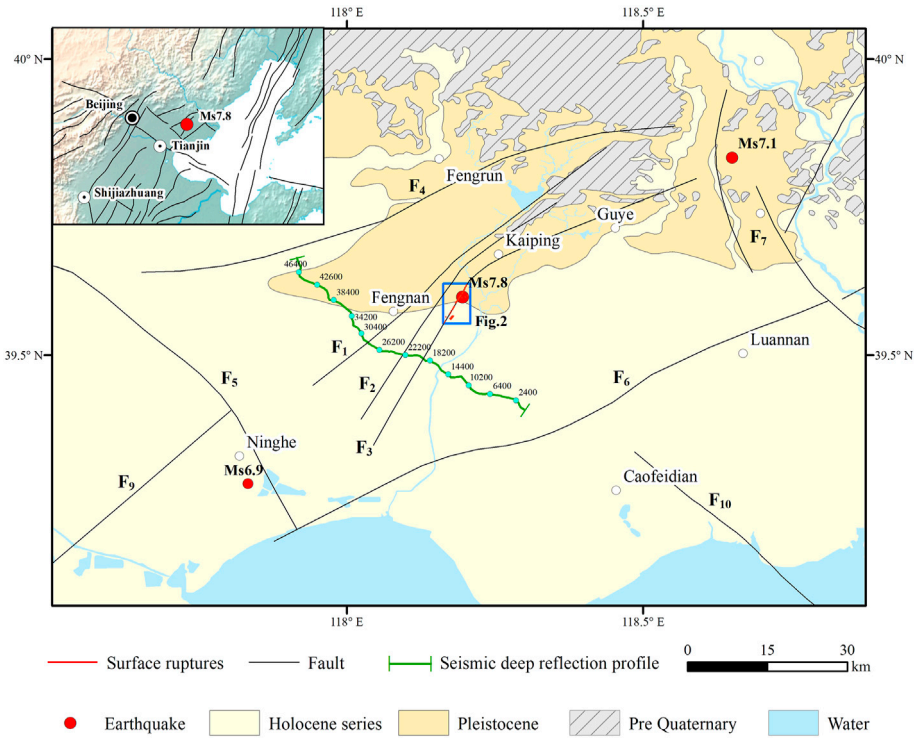

FIGURE 1
Map showing the fault distribution in the Tangshan research area in China. F_1: Douhe Fault; F_2: Weishan-Fengnan Fault; F_3: Guye-Nanhu Fault; F_4: Fengtai-Yejituo Fault; F_5: Jiyun River Fault; F_6: Ninghe-Changli Fault; F_7: Luanxian-Laoting Fault; F_8: Lulong Fault; F_9: Cangdong Fault; F_{10}: Bogezhuang Fault.

decreases from east to west but gradually increases from north to south on both sides of the Tangshan Fault.

Several active faults exist in the area. The NEE-trending Ninghe-Changli, Fengtai-Yejituo, NW-trending Luanxian-Laoting, and Jiyun River faults enclose the research area in a diamond-shaped block. The Tangshan Fault Zone forms a diagonal line across the diamond-shaped block and consists of three nearly parallel faults: the Douhe Fault (F_1), Weishan-Fengnan Fault (F_2), and Guye-Nanhu Fault (F_3) (Figure 1).

Characteristics of the shallow structure of the Tangshan earthquake seismogenic fault

Ground fissure zone

In 1976, after the Tangshan earthquake, a 10-km-long ground fissure zone (Figure 2) appeared along the Guye-Nanhu Fault (F_3), with an overall trend of N30°E and a width of ~30 m, exhibiting right-lateral strike-slip (Guo et al., 1977; Wang et al., 1981). Earthquake traces such as tensile cracks and extruded mole tracks have been found on the ground surface (Guo et al., 1977). The surface projection of the epicenter of the M_s7.8 earthquake is located above this surface rupture zone. However, the tectonic relationship between the surface rupture zone and the fault has long been debated, as have the shallow distribution characteristics of the seismogenic fault.

Previous research has conducted exploratory trench excavation across surface ruptures in the Niumaku area (Figures 3C,D) and found other ruptures resulting from an earlier earthquake (Wang et al., 1978). Moreover, exploratory trench excavation conducted at the site of the former Tangshan No. 10 Middle School (Figures 3A,B) revealed that the 1976 surface ruptures disappear at a depth of 2.3 m and do not directly penetrate the fault (Wang et al., 1978). Similarly, based on trenching near Niumaku, Wang and Li (1984) found no faults but three groups of surface ruptures at different depths. Thus, previous trenching results did not reveal the existence of seismogenic faults, especially because the depth of the trenches was too shallow to reveal fault traces at depth. The composite drilling profile at the site of the former Tangshan No. 10 Middle School revealed a near-vertical fault beneath the surface cracks, with a dip angle >83°, and a Middle Pleistocene perpendicular fault with an offset of 40 m (Liu et al., 2013).

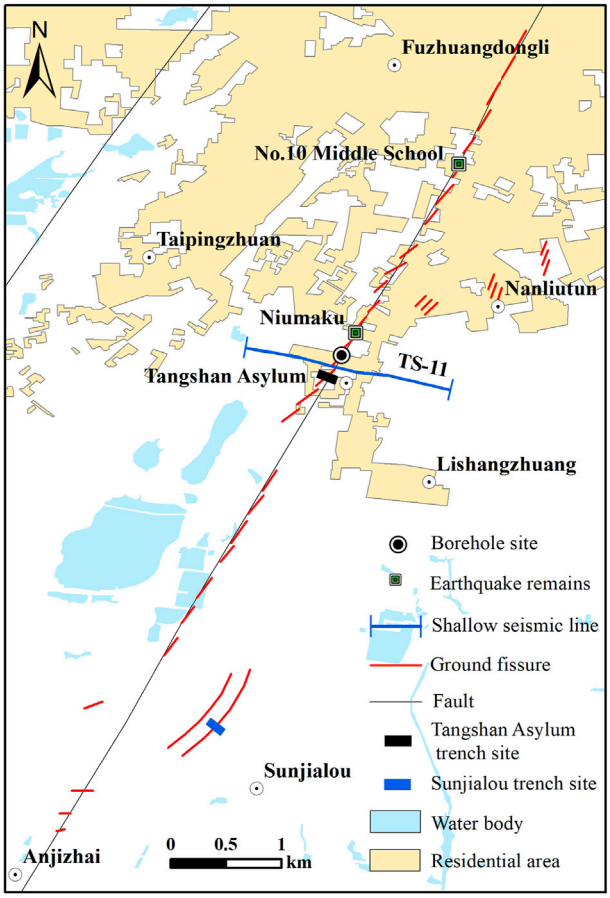

FIGURE 2
Map showing the distribution of surface ruptures and field work locations (for the location of surface ruptures, refer to Guo et al., 1977).

In recent years, trenches have been excavated beneath surface cracks in the Sunjialou area (blue rectangular area in Figure 2) (Guo et al., 2011, Guo et al., 2017; Guo and Zhao, 2019). Here, the cracks are unique, with a subsidence zone observed on the southeastern side of the right-lateral strike-slip, en-echelon surface cracks, and ~700 m long and 100 m wide (Figure 2). Guo et al. (2011) analyzed the drilling profile and trench in Sunjialou, Tangshan, and proposed that the seismogenic fault of the Tangshan earthquake was a normal fault. Extending the Sunjialou rupture to the SW connects it with one part of the Fuzhuang-Xihe subsidence zone, which also belongs to the surface rupture zone of the Tangshan earthquake, resulting in a total length >47 km (Guo et al., 2011, Guo et al., 2017; Guo and Zhao, 2019).

Three shallow artificial seismic profiles completed by our research team conducted at the location of the exploratory trench in Sunjialou revealed that the fault is located under an en-echelon–shaped surface rupture zone on the west side, with no fault present in the lower part of the trench. These results are covered in a separate article and are not discussed further here.

Shallow artificial seismic detection

A 1.6-km-long shallow seismic survey line was laid on Nanhu Avenue, 200 m south of the earthquake relic site of Niumaku (Ts-11 in Figure 2), with a wave detection distance of 3 m and a common depth point distance of 1.5 m. A near-vertical main fault (F_3) at stake No. 713 and common depth point 1,426 is interpreted as the upper breakpoint of the fault, with latitude and longitude coordinates of 39.591°N and 118.188°E.

The strongly reflected wave groups on the east side of the fault (T_1 and T_Q) are stable (Figure 4), with good continuity and level occurrence, and a decrease in depth near the fault. The T_Q wave group on the western side of the fault is also stable with good continuity. The T_1 wave group exhibits relatively poor continuity and decreases in depth at the side close to the main fault, indicating an anticline, which was likely caused by horizontal extrusion. As the fault is heavily influenced by horizontal tectonic extrusion, the occurrence of the two wave groups on both sides of the fault generally indicates an anticline, and the overall appearance of the two wave groups is almost vertical. The overall positions of T_1, T_Q, and T_N, as well as the top surface of the bedrock on the east side of the fault, are lower than those on the west side. In addition, the wave groups of the fault are offset downward. Therefore, we infer the existence of multiple branch faults that diverge upward and converge downward to the main fault.

Comparison of composite drilling profiles

Based on the location of the upper breakpoint interpreted by the shallow seismic exploration results, six field sites were selected for drilling-based exploration on the southern side of Nanhu Avenue and west of Tangshan Asylum (Figure 2). Through a comparison of key strata and an analysis of sedimentary cycles, and considering data from thermoluminescence dating, six obvious fault displacements are identified, which are 0.9, 2.1, 4.4, 5.2, 6.1, and 7.7 m from the top to bottom (Figure 5). At this site, an assemblage of gray gravel-bearing medium sand is developed at a depth of 30 m below ground. The gravel content is approximately 50%, and the gravel diameter is 1–5 cm, with good psephicity. The gravel components are predominantly limestone and quartzite and form a typical key bed with an offset of 7.7 m (Figure 5).

Thermoluminescence dating and regional data suggest that the Quaternary deposits at the site mainly developed in the Middle Pleistocene Yangliuqing Formation (Qp^2Y), the Upper

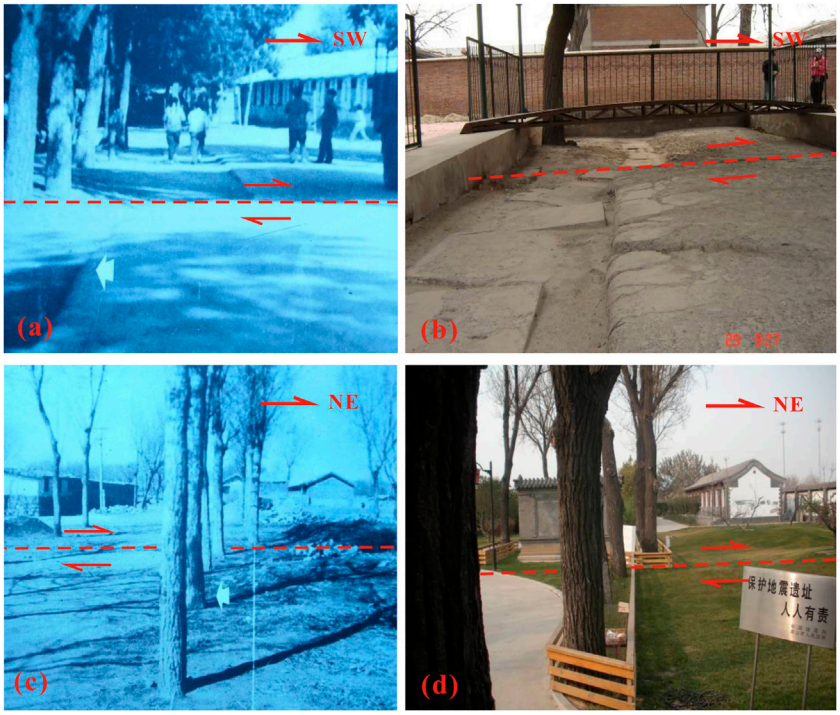

FIGURE 3
Photographs of surface ruptures. **(A)** Offset footpath with surface ruptures at the Tangshan No. 10 Middle School site, photographed after the earthquake (Fang et al., 1981); **(B)** earthquake relic site of Tangshan No. 10 Middle School; **(C)** offset trees in a yard with surface ruptures in Niumaku, photographed after the earthquake (Fang et al., 1981); **(D)** earthquake relic site at Niumaku.

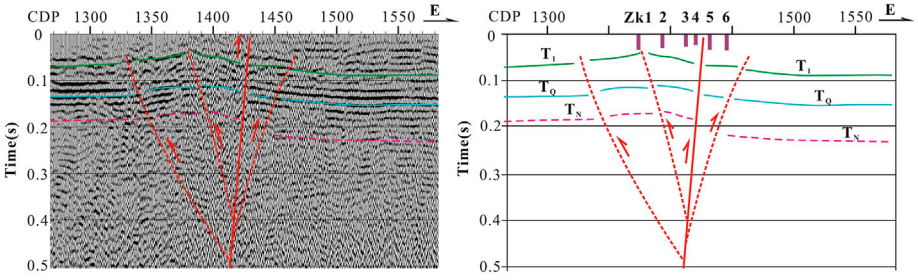

FIGURE 4
Ts-11 shallow seismic survey lines. T_1: Quaternary strong reflection interface; T_Q: bottom boundary of the Quaternary; T_N: unconformity surface at the base of the Neogene formation; CDP: common depth point.

Pleistocene Ouzhuang Formation (Qp^3O), and Holocene deposits, which are thinner and substantially influenced by human activity. It is presumed that the Ouzhuang Formation (Qp^3O) is in conformable contact with the underlying strata. The sediments are mainly brownish-yellow clay, silty clay, yellowish-brown silty sand, medium-fine sand, and medium-coarse sand and can be divided into two cycles with clear boundaries and fining-upward sequences. The upper part of the cycle is dominated by clay, the middle part by silty clay, and the lower part by fine and medium sand.

The sediments of the Yangliuqing Formation (Qp^2Y) are mainly brownish-yellow clay, silty clay, yellowish-brown to yellow silty sand, muddy silt, and grayish-yellow medium-coarse sand with a gravel layer in the lower part. Based on the sedimentary characteristics, the sediments can be divided into three cycles with clear boundaries and upward-fining sequences.

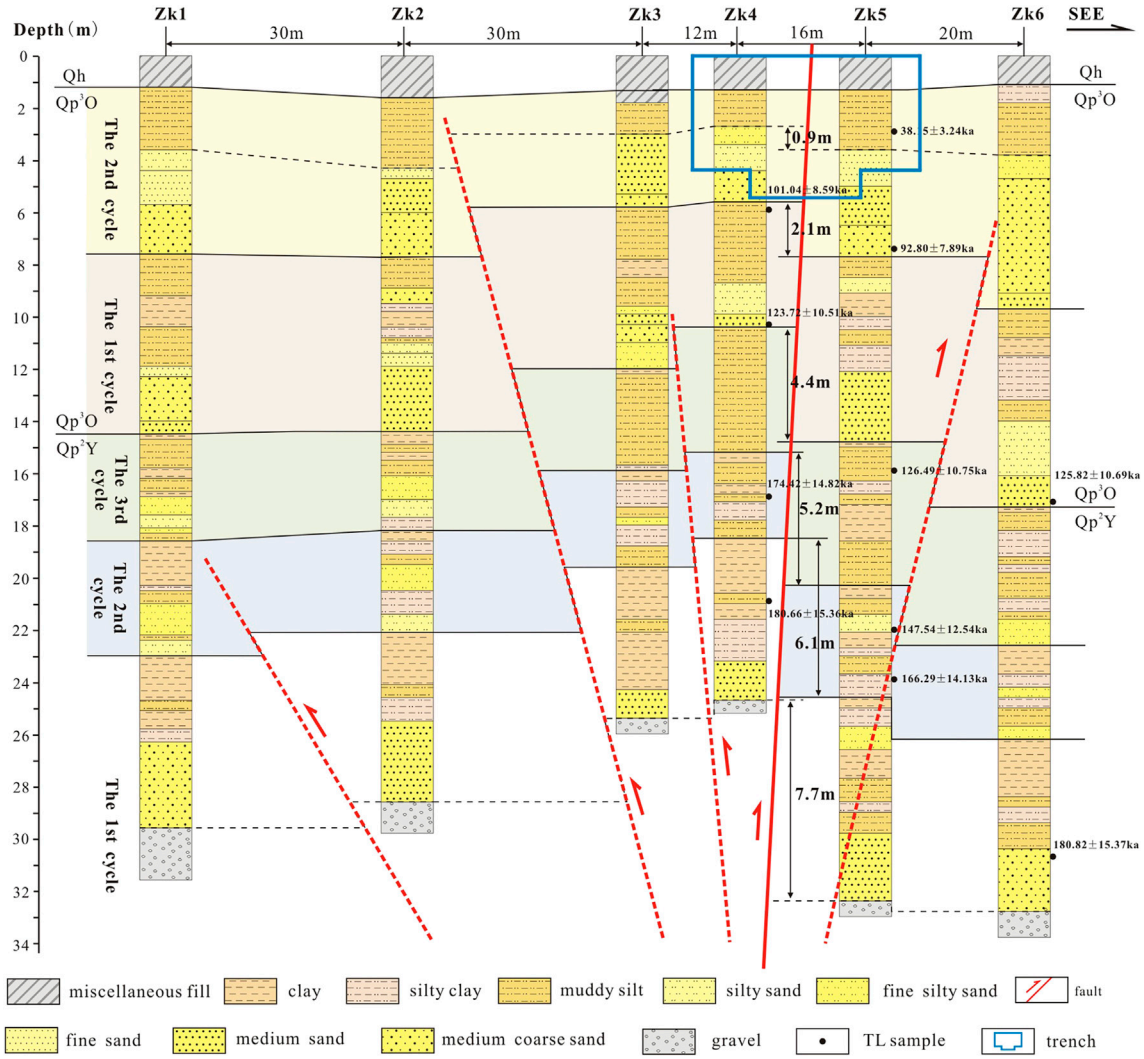

FIGURE 5
Composite drilling columnar comparison diagram at the Tangshan Asylum site.

The upper part is dominated by clay, the middle part is dominated by silty clay and muddy silt, and the lower part is dominated by fine and medium-coarse sand or gravel. The first cycle is a gravel–clay structure in its lower part, with a gravel layer at the bottom, an assemblage of dark gray fine sand in the middle, and a drop of 7.7 m at the top surface of the gravel layer. The second cycle is a structure ranging from fine silty sand to clay layers with highly variable thickness; the bottom of the east side is fine silty sand, whereas the bottom of the west side is muddy silt; the thickness of the overall breakpoint on the west side is thinner than that on the east side, and there is a 6.1 m offset between the west and east sides. The third cycle is a structure ranging from a silty sand layer to a clay layer. The average thickness of the sand layers is almost the same; however, the sand layer on the west side of the breakpoint is slightly thinner than that on the east side, and there is an offset of 5.2 m between the west and east sides.

The strata geometry and fault distribution revealed by the composite drilling profile agree with those of the shallow artificial seismic profile. The strata layers are almost horizontal but bend near the main fault. The NW side rises near the fault, whereas the SE side subsides toward the fault, resulting in a relatively significant drop. By comparing the sedimentary cycles and key strata, the composite drilling profile reveals that the main fault is located between ZK4 and ZK5. There are several fault branches on both sides of the main fault, which diverge upward and converge downward to the main fault. The overall motion of the faults is characterized by a thrust component, consistent with the shallow artificial seismic detection results.

FIGURE 6
Panoramic view of the exploratory trench at the Tangshan Asylum site.

Fault structure revealed by exploratory trench excavation

Trench characteristics

Based on the extension direction of the surface rupture zone in the Niumaku earthquake relic area and the results of shallow seismic exploration and composite drilling, the precise location of the surface rupture was obtained. Thus, an exploratory trench was excavated 300 m south of the Niumaku crack zone on the west side of Tangshan Asylum. The trench was approximately 25 m long, 13 m wide at the top, and 10 m wide at the bottom. It is a two-stage ladder-like structure, with the first stage being 5 m deep and the second stage being 1.4 m deep, with a volume of approximately 1,500 m^3 to the shallow water level (Figure 6).

The trench excavated at the Tangshan Asylum site is a large assemblage of marine sedimentary sand layers located 2–3 m below the surface, in which the distribution of faults is preserved (Figure 7). In general, although the large assemblage of loose sand layers is highly unfavorable for the construction, cleaning, and preservation of the trench, it creates unique conditions for studying the characteristics of the Tangshan Fault Zone structure, which is dominated by high-angle strike-slip movement. One of the main characteristics of the fault zone is loose marine sedimentary sand layers with small grain sizes and well-developed bedding. There are multiple types of bedding, such as horizontal bedding, massive bedding, and planar cross-bedding, which can completely record and clearly identify small fault movements. This is an advantage that is not often available in trenches elsewhere. Another major characteristic is that mud was drawn into the main faults with relatively large-scale slippage during the rupture process. As the loose marine sedimentary sand layers around the faults are gradually exposed, these main faults become especially prominent (Figure 8B).

Multiple fault branches were revealed by the trench, which provide more structural information. The trench was carefully cleaned and cataloged, and each fault branch was numbered and classified (Figure 7) to best reflect the true traces of the faults. The upper part of the trench was divided into the following five stratigraphic units from top to bottom (Figure 7):

① Artificial fill, containing coal cinder, bricks, and other construction waste.
② Dark gray cultivated soil, with two groups of ground cracks of different timings, developed in the upper and lower layers, representing two separate earthquake events (Liu et al., 2013).
③ Yellowish-gray silty clay, whose sand content gradually increases from top to bottom and gradually changes to yellowish-brown. A large number of cracks are observed in the upper part. This layer contains some sole-shaped black blocks in the south wall, with some white calcareous nodules in the middle that absorb black substances such as carbon and manganese (Figure 9).
④ A cinerous mud layer, with a uniform composition, shows strong water absorption in the lower part. This layer is divided into upper and lower groups in the north wall of the trench. Despite having the same composition, the upper group is greenish, whereas the lower group is cyan. In the depression at the eastern end of the south wall, there are several assemblages of thin, muddy layers whose color gradually changes from green to cyan; these can be divided into four assemblages of thin layers.
⑤ A large assemblage of fine silty sand layers with various types of marine sediment structures, such as cross-bedding, parallel bedding, and horizontal bedding. The sandstone body is grayish-yellow, dry, and loose.

The lower part of the trench is a large assemblage of fine silty sand layers (layer ⑤), which can be subdivided into the following five stratigraphic units from top to bottom (Figure 7):

⑤-1: A grayish-yellow silty sand layer characterized by horizontal bedding.
⑤-2: A grayish-yellow sandy gravel layer characterized by planar cross-bedding; gravel is arranged in a specific direction, with a diameter of 0.3–1.0 cm.
⑤-3: A yellowish-brown fine silty sand layer, with no clear bedding, showing good consolidation. In the south wall of the trench, a layer of gravel is present at the bottom of this layer, arranged in a specific direction, with a diameter of 0.5–5.0 cm.
⑤-4: A grayish-yellow silty sand layer characterized by inclined bedding containing a gravel layer, with gravels arranged in a specific direction and a gravel diameter of 0.3–1.0 cm. Occasionally, large gravels with diameters of 2–5 cm were observed in the southeast wall. The south wall

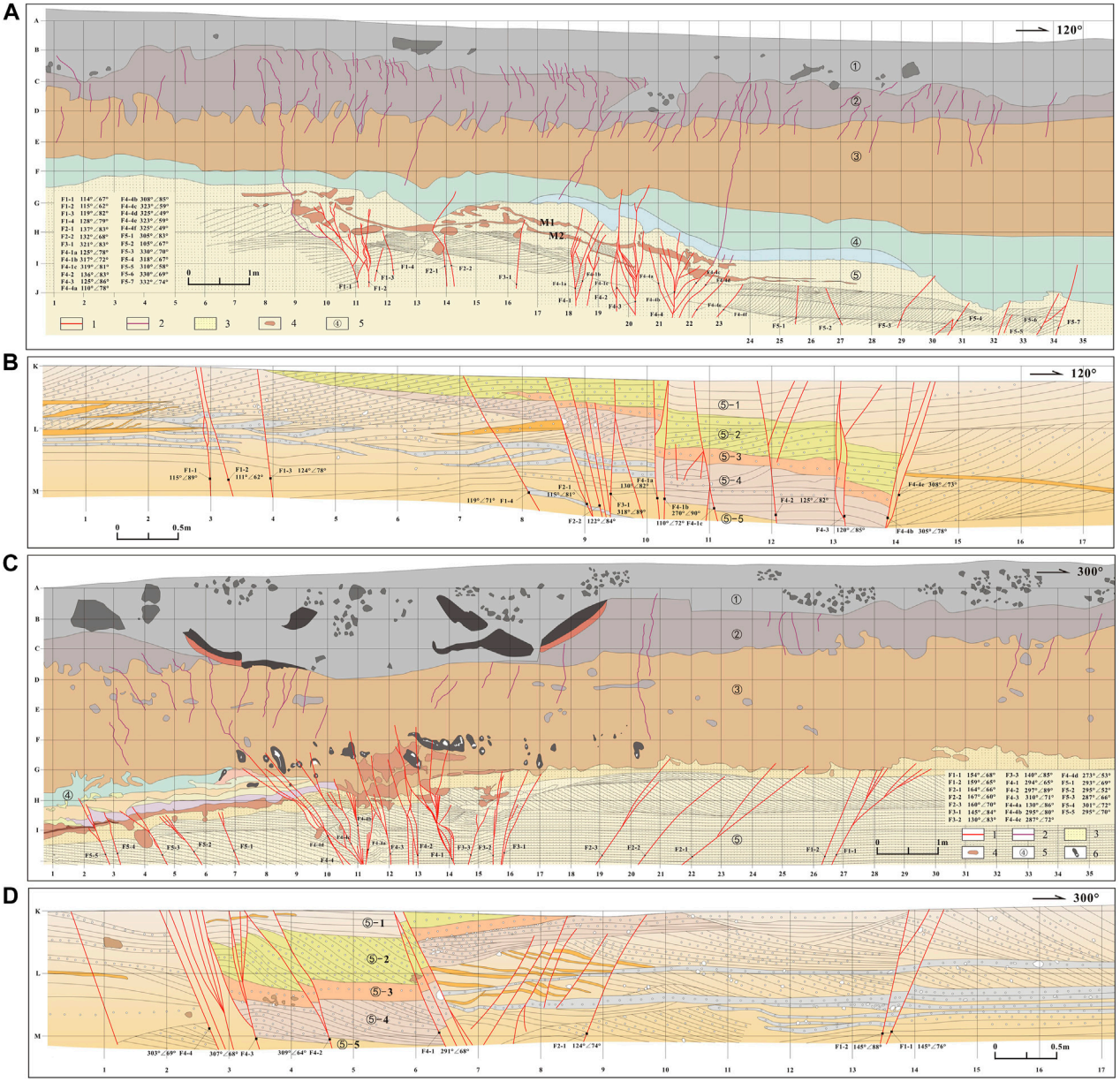

FIGURE 7
Sections of the exploratory trench at the Tangshan Asylum site. **(A)** Section of the upper part of the north wall; **(B)** section of the lower part of the north wall; **(C)** section of the upper part of the south wall; **(D)** section of the lower part of the south wall. 1: fault; 2: cracks; 3: large assemblage of fine silty sand layers; 4: brown boulder clay; 5: strata layer number; 6: sole-shaped black block with white calcareous nodules.

of the trench clearly shows that the fault offsets a piece of boulder clay with a diameter of ~10 cm (Figure 7D).

⑤-5: A grayish-yellow silty sand layer dominated by planar cross-bedding, with horizontal bedding and wedge-shaped bedding developed in between. In the southeast wall of the fault, there are several yellowish-brown thin, muddy silt layers that are offset by the fault zone, indicative of a normal fault.

Fault structural features

A large number of cracks are observed near the surface of the trench, divided into two layers, consistent with previous studies (Wang et al., 1978, Wang et al., 1984). The upper layer of the SE-trending cracks is covered by miscellaneous surface fill, presumably caused by the 1976 Tangshan earthquake.

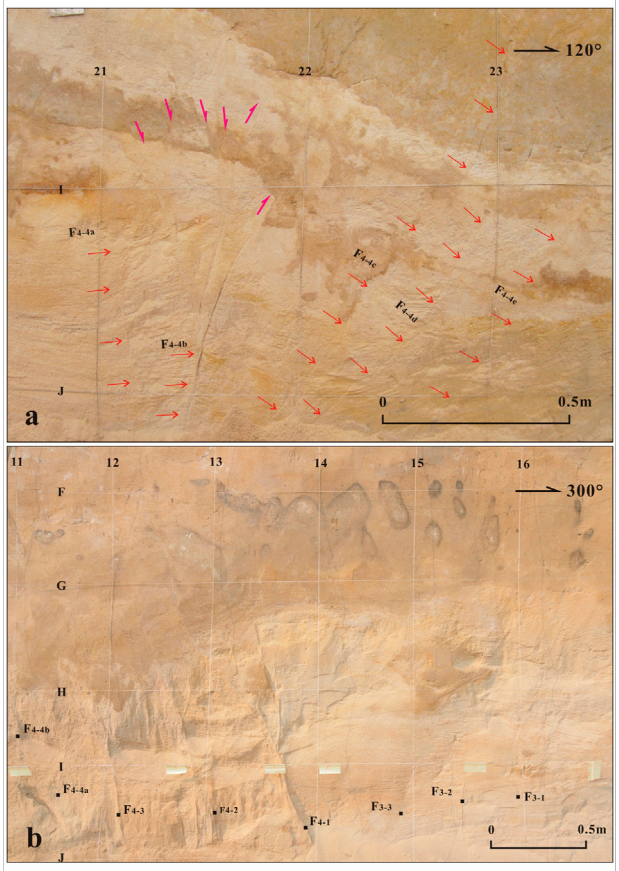

FIGURE 8
Photographs of the exploratory trench (partial images): **(A)** grid range (21–23, (I–J) of the north wall and **(B)** grid range (11–16, (F–I) of the south wall.

Two assemblages (M_1 and M_2) of grayish-brown thin mud layers occur in the north wall (Figure 7A; Figure 10B) and are repeatedly offset by the faults. Conversely, only one assemblage of grayish-brown thin mud layers has developed at the east end of the south wall (M), which is offset by the fault into multiple small mud blocks within grids 10–14 (Figure 7C).

The fault groups revealed by the trench diverge upward and can be divided into five groups, F_1 to F_5, each of which can be further subdivided. Among them, the F_4 fault group has the densest fault branches, concentrated in the center of the trench. The F_4 fault group in the north wall is concentrated in the upper grids 18–24 and the lower grids 10–15; in the south wall, the F_4 fault group is concentrated in the upper grids 9–15 and the lower grids 2–7 (Figure 7). The fault group F_4 corresponds to the main fault and can be subdivided into F_{4-1} to F_{4-6} in the upper part of the north wall, among which the fault F_{4-4} is relatively complex, diverging upward and converging downward into a fault; F_{4-4} can be further subdivided into F_{4-4a}, F_{4-4b}, F_{4-4c}, F_{4-4d}, and F_{4-4e} (Figure 8A). There is clear offset and traction deformation in the strata near the fault. In the upper part of the south wall, the fault group F_4 is also subdivided into F_{4-1}, F_{4-2}, F_{4-2}, and F_{4-4}, among which the fault F_{4-4} is composed of multiple small faults that intersect and converge. Here, F_{4-4} is further subdivided into F_{4-4a}, F_{4-4b}, F_{4-4c}, and F_{4-4d} (Figure 8B).

The number of fault branches is equivalent in the upper and lower parts, as well as in the north and south walls of the trench. Figure 10 shows photographs of the numbered faults in the upper and lower parts of the trench. We selected grids 8–11 on the north wall in the lower part of the deep trench and excavated a horizontal trench on its upper platform to reveal the horizontal extension direction of the fault group and determine the corresponding relationship between the lower fault in the small trench and the upper fault. This analysis confirmed fault branch numbering.

The trench reveals a large number of fault branches and cracks, which exhibit good regularity and diverge upward. The strata at the same level are higher in the west and lower in the east, with nearly vertical faults in the center, exhibiting strong strike-slip features (Figures 9B,E). The central faults gradually undergo a transition westward into fault branches dominated by normal fault components (Figures 9A,F) and eastward into fault branches dominated by thrust components (Figures 9C,D). The amount of perpendicular offset between the fault branches at both ends is <5 cm. The closer to the central main fault, the clearer the fault plane and the larger the dislocation. The sedimentary sand layers on both sides of the central main fault are completely different, showing strong characteristics of the strike-slip movement. The fault distribution characteristics revealed by the trench at the Tangshan Asylum site are similar to a flower structure and are the most significant structural features in the shallow part of the Tangshan Fault Zone.

Discussion

Kinematic characteristics of the seismogenic fault

The movement characteristics of the seismogenic fault of the Tangshan earthquake have long been debated, with previous research suggesting a right-lateral strike-slip fault (Qiu, 1976; Zhang et al., 1980), a right-lateral strike-slip fault with a normal component (Hao and You, 2001), a high-angle thrust fault (You et al., 2002; Liu et al., 2013), or a normal fault (Qiu et al., 2005; Guo et al., 2011, Guo et al., 2017). All of these interpretations were obtained from a single detection method, which is highly limiting for an earthquake as complex as the Tangshan event. Therefore, it is necessary to integrate multiple detection methods for a more thorough analysis. This study combined analyses of surface ruptures, exploratory trenches, composite drilling columnar profiles, shallow seismic profiles, and focal

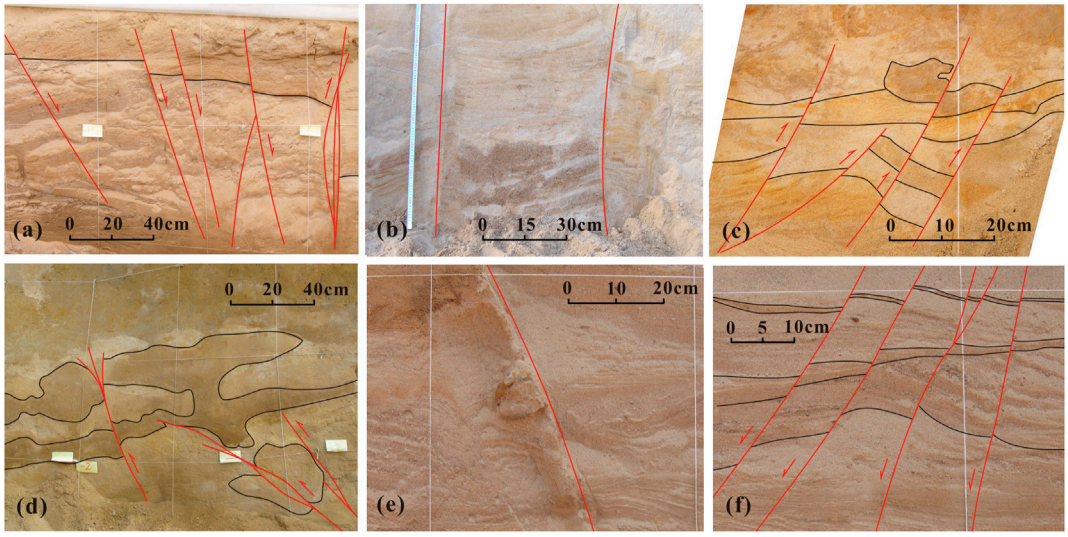

FIGURE 9
Fault patterns in the trench. **(A)** Normal faults in the western part of the north wall (specific location shown in grids 8–10 in Figure 7B); **(B)** strike-slip faults in the middle part of the north wall (specific location shown in grids 16–19 in Figure 7A); **(C)** thrust faults in the eastern part of the north wall (specific location shown in grids 34–35 in Figure 7A); **(D)** thrust faults in the eastern part of the south wall (specific location shown in grids 2–5 in Figure 7C); **(E)** strike-slip faults in the middle part of the south wall (specific location shown in grids 6–7 in Figure 7D); **(F)** thrust faults in the eastern part of the south wall (specific location shown in grids 7–8 in Figure 7C).

mechanism solutions to comprehensively evaluate the kinematic characteristics of the Tangshan earthquake seismogenic fault.

After the M_s7.8 Tangshan earthquake in 1976, a 10-km-long surface rupture zone (Figure 2) appeared in the meizoseismal area along the Tangshan-Guye Fault (F_3) (Guo et al., 1977). The two sides of the rupture exhibit horizontal deformation in a right-lateral manner. The rupture zone is composed of no more than 20 deformed cracks in an en-echelon structure in the reverse direction. The maximum horizontal right-lateral offset is 2.3 m. The NW side rises relative to the center, whereas the SE side subsides by 0.2–0.7 m.

Previous research on the surface rupture zone (Guo et al., 1977) coupled with the large-scale "M_s7.8 Tangshan Earthquake Seismogenic Structure Map (1:1,000)" obtained from the Hebei Earthquake Agency reveals that the surface rupture zone conforms to the Riedel shear model. The strike of the surface rupture zone is NE30°, with a relatively well-developed R shear that moves in a direction of 45–60°. Moreover, a small number of push-ups with a long axis direction of 150° also exist. Riedel shears are closely related to the earthquake rupture mechanism (Tchalenko, 1970; Tchalenko and Ambraseys, 1970; Aydin and Page, 1984). Laboratory experiments and field-based seismic surface rupture investigations have shown that Riedel shears are the main type of initial rupture for seismic faults, especially regarding the surface rupture of large strike-slip earthquakes (Tchalenko, 1970; Tchalenko and Ambraseys, 1970; Deng and Zhang, 1984; Bergerat et al., 2003; Lin et al., 2004, Lin et al., 2011; Rao et al., 2011; Li et al., 2015; Liu et al., 2021). This also explains why the series of cracks observed in the trench do not break through the surface but are instead typical surface ruptures characterizing strike-slip earthquakes.

After the trench excavation at the Tangshan Asylum site, a parallelepiped was identified in the marine fine silty sand layer in the north wall (Figure 11). This parallelepiped is brownish-yellow, cemented by silt and mud, hard, and regular in shape, located in the gray-white marine fine silty sand layer 4 m below the ground surface, where the sand body has clear bedding and a uniform texture and is not affected by human activities (Figures 11A,B). This feature is located in the fault zone and is presumably caused by long-term creep along the fault. The boulder clay has a standard positive torsion geometrical shape, and the response fault exhibits right-lateral strike-slip motion (Figures 11C–E).

At the earthquake relic site of the Tangshan No. 10 Middle School, seven holes were drilled close together across the surface rupture over 22 m, with the deepest hole being 106 m. These revealed that the main fault has a dip angle >83° (Liu et al., 2013). The shallow seismic profile (TS-11) reveals multiple fault branches and the high dip angle of the main fault. The trench reveals that the main fault group (F_4) has a high dip angle, most fault branches have dip angles >80° (Figure 7), and the faults diverge upward and converge downward toward the main fault, which is almost vertical, with clear strike-slip and vertical offsets (Figure 9).

Based on initial motion P-wave data for the 1976 M_s7.8 Tangshan earthquake collected from seismic stations around the world, the calculated focal mechanism

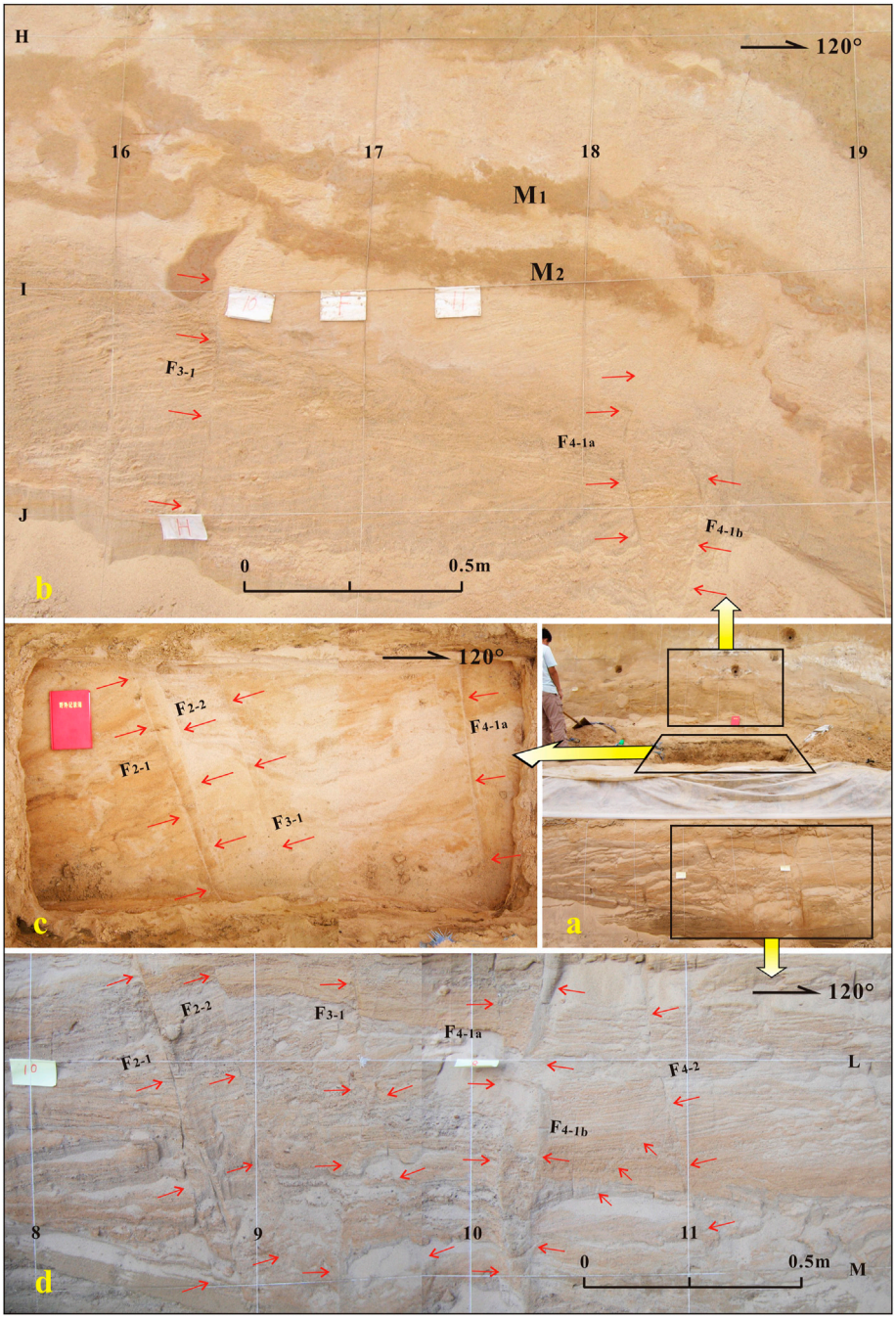

FIGURE 10
Fault relationships revealed in the upper part of the north wall of the exploratory trench and deep trench. Photographs showing **(A)** the north wall of the exploratory trench and deep trench, **(B)** part of the north wall, **(C)** the exploratory trench in the horizontal direction, and **(D)** part of the north wall of the deep trench.

solutions are similar. The Tangshan earthquake manifested as a high-dip, right-lateral, strike-slip earthquake (Qiu, 1976; Butler et al., 1979; Zhang et al., 1980; Nabelek et al., 1987; Shedlock et al., 1987; Huang and Yeh, 1997). Bulter et al. (1979) also analyzed the far-field body waves and surface waves of the earthquake, and through fitting inversion of synthetic seismic waveforms and observational records, they suggested that the main shock of the Tangshan earthquake was a complex faulting sequence composed of several events, including strike-slip and thrust events.

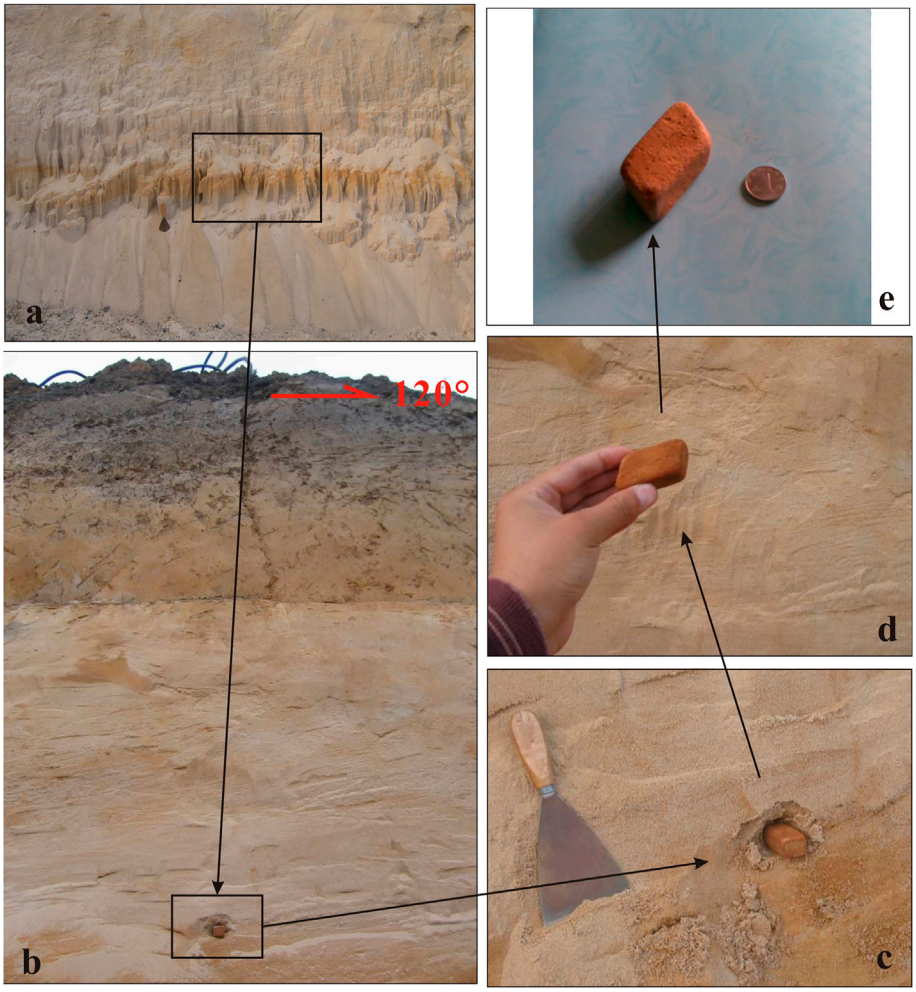

FIGURE 11
Photographs of parallelepiped boulder clay samples in the north wall of the exploratory trench. **(A)** Sand layer before cleaning; **(B)** sand layer after cleaning; **(C)** sample *in situ*; **(D)** specific sample shape; **(E)** surface of the preserved boulder clay with longitudinal cracks.

Based on these results, we suggest that the Guye-Nanhu Fault (F_3), which represents the shallow response to the seismogenic structure of the Tangshan earthquake, is characterized by right-lateral strike-slip movement with a thrust component and an almost vertical fault plane.

Deep and shallow structural model of the seismogenic fault

The en-echelon–shaped surface rupture zone is characterized by right-lateral strike-slip motion. The shallow seismic profile (TS-11) and the composite drilling columnar profile obtained at the Tangshan Asylum site reveal that there is an almost vertical main fault in the lower part of the surface rupture zone, where there is a clear perpendicular offset. Furthermore, multiple fault branches diverge upward and converge downward to the main fault, conforming to a typical positive flower structural model.

The trench excavated at the Tangshan Asylum site reveals the specific shape of the faults, which are characterized by a combination of fault branches that tend to diverge outward like a flower. The normal fault branches also become progressively steeper with depth and converge downward to the vertical main strike-slip fault with a deep-cut basement. A vertical dislocation occurs between the two sides of the fault zone, where the west side rises but the east side subsides, relative to the fault zone. The central faults are dominated by strike-slip motion. The fault branches to the west are predominantly normal faults, whereas those to the east are reverse faults, and those close to the central faults are strike-slip faults. The farther the faults are to the west and east, the gentler the dip angle is and the clearer the normal and reverse faulting components are. The profile is

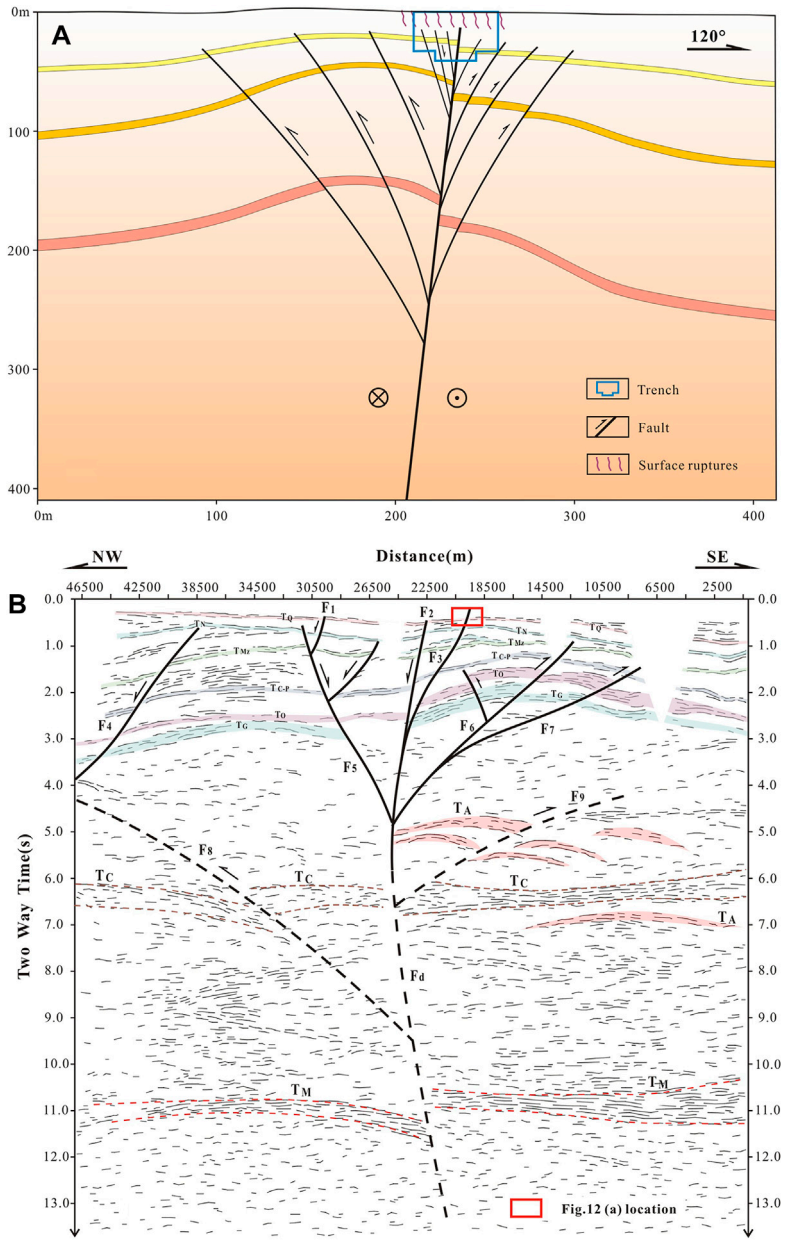

FIGURE 12
Schematic representation of the seismogenic fault of the Tangshan earthquake: **(A)** shallow part of the seismogenic fault and **(B)** deep seismic reflection profile across the Tangshan Fault Zone in the south (adapted from Liu et al., 2011).

characterized by a combination of fault branches diverging outward like a flower. Again, the fault branches become progressively steeper with depth and converge downward to the vertical main strike-slip fault. The trench excavated at the Tangshan asylum site reveals a unique structural model, which is confirmed by the composite drilling columnar profile and the shallow seismic exploration results. Figure 12A shows a model of the shallow structure of the seismogenic fault of the Tangshan earthquake, which manifests as a positive flower structure. A high-angle thrust fault is located to the west of the main fault, and a series of tensile normal faults appear in front of the high-angle thrust faults, owing to surface tension and other factors, for example, the normal faults in the western section of the exploratory trench.

A 49.4-km-long deep seismic reflection profile with a line of measurement perpendicular to the Tangshan Fault Zone was completed by our research team (Figure 1). T_Q, the reflection wave on the profile, is interpreted as bottom boundary reflections

of the Quaternary overburden, T_N as the bottom boundary of the Neogene stratum, T_{Mz} as the bottom boundary of the Mesozoic stratum, and T_O and T_{C-P} as reflections of the Paleozoic Ordovician, Carboniferous, and Permian strata, respectively; the reflection wave group T_C is the reflection from the upper and lower crustal partition interface, while T_M is the reflection from the crust–mantle transition zone; T_A is interpreted as seismic multi-arch structures.

The deep crustal fault, F_d, revealed by the deep seismic reflection profile is located below line stake No. 22500 (Figure 12B). There are obvious transverse discontinuities in the upper and lower crustal partition interface reflection T_C and the crust–mantle transition zone reflection T_M near the deep fault, and the interface occurrence and wave characteristics of the lower crustal reflection on both sides are also clearly different. Thus, F_d is shown to be a deep fault between the upper and lower crustal partition and the Mohorovicic discontinuity. The existence of this deep fault provides conditions for the upwelling of thermal materials in the upper mantle and intracrustal tectonic deformation.

The T_c interface on the west side of deep fault F_d presents a subducting underthrust feature; therefore, we suppose that there is an F_8 fault. There is a clear overlap of arcuate tectonic features at the bottom of the upper crust, suggesting the existence of an F_9 fault. These two faults merge downward over the deep fault F_d.

Faults F_1–F_3, as revealed by the deep seismic reflection profile, correspond to three branching faults of the Tangshan Fault Zone. F_5–F_7 extend downward at different dips in the profile and converge at a depth of approximately 10 km to form an almost upright fault inserted into the upper crustal floor, near the upper and lower crustal partition interface, which may be associated with the deep fault of the Mohorovicic discontinuity. The shallow seismic exploration, drilling, and excavated trench area is located near the epicenter, while the 2D deep seismic reflection line is 13.1 km from the epicenter. Therefore, there may be inconsistencies in the deep and shallow survey results in terms of structural details, but the general form should be consistent.

A deep crustal fault provides the deep power source for the Tangshan earthquake. The deep tectonic form revealed by the deep seismic reflection profiles further supports the superficial tectonic model. This complex system of deep and shallow faults constitutes the tectonic background of the Tangshan earthquake. In summary, there is a main upright strike-slip fault, deep in the basement beneath the Tangshan Fault Zone, which faults the Mohorovicic surface. The branching faults are gentle on the top and steep on the bottom and converge downward to the main fault, displaying different occurrence characteristics owing to the influence of the stress field in different geological periods. The Tangshan Fault Zone is characterized by right strike-slip movement under the near-NEE stable stress field (Wan, 2007) during the Neotectonic period (since 0.78 Ma). A large number of detailed survey works reveal that the faults are characterized by a flower-like combination of branching reverse faults that spread outward at the shallow section, with the branching reverse faults gentle on the top and steep on the bottom, protruding inward and converging downward to the main strike-slip faults. These features form a positive flower-like tectonic structure overall (Figure 12A).

Newly generated fault zone in North China

The North China Plain fault basin is bounded by the Yanshan uplift, the Taihang uplift, the Luxi uplift, and the Tanlu Fault Zone (the Ludong and Liaodong uplifts). The NNE-oriented Tanlu Fault Zone is a large-scale and structurally complex fault zone in eastern China, cutting through the lithosphere for over 3,500 km (Wan, 1996) and dominating the eastern boundary of the North China Plain faulted basin together with the Ludong and Liaodong uplifts (Figure 13).

Between 1966 and 1976, the Xingtai M_s7.2, Hejian M_s6.3, and Tangshan M_s7.8 earthquakes occurred in the North China Plain region in sequence from north to south. Previous work has indicated the existence of a newly generated fault zone that began to develop in the Neogene based on the linear alignment of seismotectonics (Xu et al., 1996). In this study, we focused on exploring the mechanism of the formation of the Tangshan–Hejian–Xingtai Neotectonic zone from the perspective of the dynamics of the Tangshan earthquake.

Angular unconformities between structures of the Early and Middle Pleistocene are widespread in mainland China, and the characteristics of tectonic activity since the Middle Pleistocene are generally consistent. The horizontal principal stress during the Neotectonic period (since 0.78 Ma) is in the near-NEE direction in northern China (Wan, 2007). In this tectonic setting, most of the pre-existing high-dipping faults in the upper crust of mainland China happen to intersect the maximum principal compressive stress direction almost perpendicularly or at large angles; therefore, the fault surfaces are extruded relatively tightly. Their activity often shows a certain left or right strike-slip characteristic because of the different angles between the direction of maximum principal stress and the fault plane. The northern section of the Tanlu Fault Zone is extruded in the NNE direction, while the southern section is extruded in the near east–west direction, presenting a reverse fault with a slight right strike-slip (Wan 1996).

The near-NEE–oriented stress field direction in North China and the lower strike-slip component of the Tanlu Fault Zone result in stress accumulation within the North China Plain faulted basin. The middle of this basin is approximately rectangular (Figure 13, blue dashed box), and the Tangshan–Hejian–Xingtai Fault Zone is located exactly at the diagonal position of the rectangle, which means that faults are easily developed.

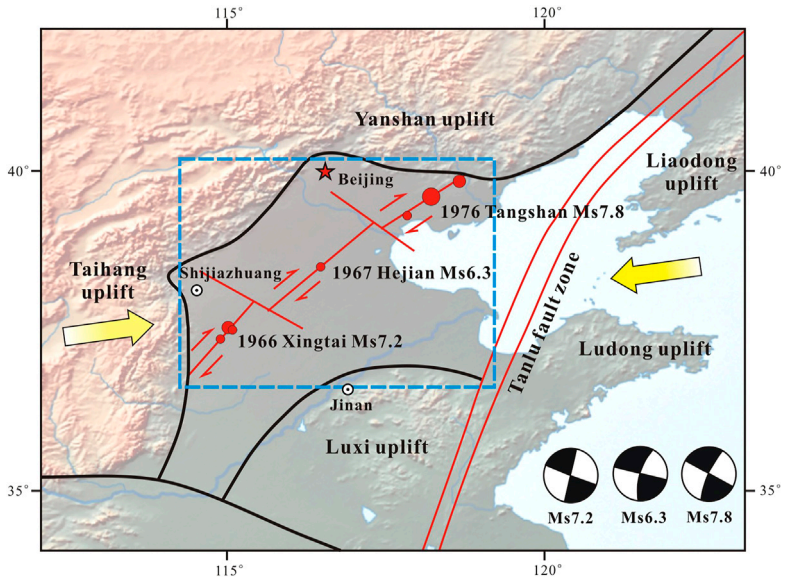

FIGURE 13
Tectonic map of the North China Plain faulted basin (focal mechanism solutions according to Xu et al., 1996; stress field according to Wan, 2007).

Based on the data from small seismic positioning, petroleum seismic profiles, and deep seismic reflection profiles, the Tangshan–Hejian–Xingtai Fault Zone is speculated to be a newly generated seismotectonic zone with a length of 500 km, which is oblique and shows a gradual change in fault orientation from near-NNE to near-NE from south to north, similar to the change in focal mechanism solutions (Figure 13).

Deep physical survey data reveal the existence of a buried fault from the focal location to the Mohorovicic discontinuity below the epicenter of the 1976 Xingtai earthquake, which is a high-dip supracrustal fault (Wang et al., 1993) similar to the deep fault of the Tangshan earthquake. Both are large ultracrustal deep faults.

The Tangshan Fault Zone is the largest in tectonic scale, and several paleoseismic events, characterized by alternating periods of relatively intensive earthquakes and quiet periods (Liu et al., 2013), have occurred along this section since the Middle Pleistocene. Therefore, the Tangshan Fault Zone can be presumed as the first active section. No tectonically significant surface fault zones have been found in the Xingtai earthquake, and there are only a few paleoseismic studies. Xu et al. (2000) suggested that the Xingtai earthquake fault was a new fault in the process of upward extension. The available research on the Hejian earthquake is least among these earthquakes. Throughout history, no $\geq M_s7$ earthquakes have occurred in the Hejian area, although it is speculated to be a seismic hazard section in the future. The inconsistency of the seismic activity characteristics of different sections also indicates that the fault zone is gradually penetrating and has a clear Neogenic nature.

The frequent occurrence of aftershocks during the 55 years after the Xingtai earthquake and the 45 years after the Tangshan earthquake further suggests that this is a gradually penetrating Neogenic fault zone. Therefore, this fault zone is assumed to have experienced overall faulting from south to north during the 10-year period from 1966 to 1976. The Tangshan and Xingtai sections have already experienced earthquakes of magnitude 7 or greater; therefore, the risk of earthquakes of magnitude 7 or greater occurring in the Hejian section is high. Yin et al. (2015) comprehensively examined historical earthquake records and paleoearthquake research achievements in the North China basin and suggested that there is an earthquake gap between Hejian and Tianjin along the "Tangshan–Hejian–Cixian" right strike-slip fault zone, which is consistent with our conclusions.

Conclusion

(1) Based on analyses of surface ruptures, exploratory trenches, composite drilling columnar profiles, shallow seismic profiles, and focal mechanism solutions, our study indicates that the NNE-trending Guye-Nanhu Fault represents the shallow response to the seismogenic structure of the Tangshan earthquake. This fault has an almost vertical dip and NW-trending main fault direction with characteristics of thrust movement.
(2) The trench excavated at the Tangshan Asylum site reveals a large number of fault branches and cracks under the surface

rupture, which are highly regular and diverge upward. The strata at the same layer are higher in the west and lower in the east, with nearly vertical faults in the center, exhibiting strong strike-slip features. The central faults gradually transition westward into fault branches dominated by normal faulting components, transition eastward into fault branches dominated by thrust components, and converge downward to the near-vertical main strike-slip fault. There is a vertical offset between the two sides of the fault zone, with the west side rising and the east side subsiding. The central faults are dominated by strike-slip motion. The fault branches on the west are predominantly normal faults, those on the east are reverse faults, and those close to the central faults are strike-slip.

(3) Shallow seismic exploration profile, composite drilling columnar profile, and exploratory trench data reveal that the shallow structure of the seismogenic fault of the 1976 Tangshan earthquake conforms to a positive flower structure model, where the profile is characterized by a combination of reverse fault branches diverging outward like a flower. The reverse fault branches become progressively steeper with depth, bulge inward, and converge downward to the vertical main strike-slip fault, typically forming a positive horst-shaped structural pattern. A high-angle thrust fault is located to the west of the main strike-slip fault, and a series of tensile normal faults appear in front of the high-angle thrust fault, owing to local tension and other factors; this corresponds to the small normal fault group in the western section of the trench. The tectonic form revealed by the deep seismic reflection profiles further supports the superficial tectonic model.

(4) Based on the linear alignment of regional seismic tectonics, the newly generated Tangshan–Hejian–Xingtai Fault Zone is speculated to exist, with a length of 500 km and an oblique alignment. The near-NEE orientation of the stress field in North China and the lower strike-slip movement component of the Tanlu Fault Zone have led to easy faulting in the Tangshan–Hejian–Xingtai Fault Zone, which lies diagonally in the middle rectangular area of the North China Plain faulted basin. The inconsistency of the seismic activity in different sections also indicates that the fault is gradually penetrating and has a distinct Neogenic nature. Earthquakes of magnitude 7 or greater have already occurred in the Tangshan and Xingtai sections; therefore, there is a relatively high risk of earthquakes of magnitude 7 or greater occurring in the Hejian section.

Data availability statement

The raw data supporting the conclusions of this article will be made available by the authors, without undue reservation.

Author contributions

KL and YL contributed to the conception and design of the study. KL completed the trenching and drilling work and wrote the first draft of the manuscript. BL completed seismic deep reflection interpretation. WW completed shallow seismic exploration. YN completed the drawing. YL, YN, and WW wrote sections of the manuscript. All authors contributed to manuscript revision and read and approved the submitted version.

Funding

This research was financially supported by the National Natural Science Foundation of China (Grant No. 41631073) and the Opening Foundation of Hebei Key Laboratory of Earthquake Dynamics (Grant No. FZ212101).

Acknowledgments

The authors thank Guosheng Qu and Jianqiang Chen for their help with field work.

Conflict of interest

WW was employed by Xi'an Research Institute Co., Ltd., China Coal Technology and Engineering Group Corp.

The remaining authors declare that the research was conducted in the absence of any commercial or financial relationships that could be construed as a potential conflict of interest.

Publisher's note

References

An, M. J., Feng, M., and Zhao, Y. (2009). Destruction of lithosphere within the north China craton inferred from surface wave tomography. *Geochem. Geophys. Geosyst.* 10, 1–18. doi:10.1029/2009gc002562

Aydin, A., and Page, B. (1984). Diverse pliocene-quaternary tectonics in a transform environment, san francisco Bay region, California. *Geol. Soc. Am. Bull.* 95, 1303. doi:10.1130/0016-7606(1984)95<1303:dptiat>2.0.co;2

Bao, F., Li, Z. W., Tian, B. F., Wang, L. L., and Tu, G. H. (2019). Sediment thickness variations of the Tangshan fault zone in North China from a dense seismic array and microtremor survey. *J. Asian Earth Sci.* 185, 104045. doi:10.1016/j.jseaes.2019.104045

Bao, F., Li, Z. W., Shi, Y. T., Tian, B. F., Chong, J. J., Rong, W. J., et al. (2021). Sediment structures constrained by converted waves from local earthquakes recorded by a dense seismic array in the Tangshan earthquake region. *Pure Appl. Geophys.* 178, 379–397. doi:10.1007/s00024-021-02667-5

Bao, F., Li, Z. W., Yuen, D. A., Zhao, J. Z., Ren, J., Tian, B. F., et al. (2018). Shallow structure of the Tangshan fault zone unveiled by dense seismic array and horizontal-to-vertical spectral ratio method. *Phys. Earth Planet. Interiors* 281, 46–54. doi:10.1016/j.pepi.2018.05.004

Bergerat, F., Angelier, J., Gudmundsson, A., and Torfason, H. (2003). Push-ups, fracture patterns, and palaeoseismology of the Leirubakki fault, South Iceland. *Journal of Structural Geology* 25 (4), 591–609. doi:10.1016/S0191-8141(02)00051-2

Butler, R., Stewart, G., and Kanamori, H. (1979). The July 27, 1976 Tangshan, China earthquake-A complex sequence of intraplate events. *Bull. Seismol. Soc. Am.* 69, 207–220. doi:10.1785/bssa0690010207

Deng, Q. D., and Zhang, P. Z. (1984). Research on the geometry of shear fracture zones. *J. Geophys. Res.* 89, 5699–5710. doi:10.1029/jb089ib07p05699

Fang, H. Q., Wang, Z. Q., and Zhao, S. D. (1981). *Approach to Tangshan earthquake engineering geological problems*. Beijing: Chinese Academy Building Research Press.

Guo, H., Jiang, W. L., and Xie, X. S. (2011). Late-Quaternary strong earthquakes on the seismogenic fault of the 1976 Ms7.8 Tangshan earthquake, Hebei, as revealed by drilling and trenching. *Sci. China Earth Sci.* 54, 1696–1715. doi:10.1007/s11430-011-4218-x

Guo, H., Jiang, W. L., and Xie, X. S. (2017). Multiple faulting events revealed by trench analysis of the seismogenic structure of the 1976 Ms7.1 Luanxian earthquake, Tangshan Region, China. *J. Asian Earth Sci.* 147, 424–438. doi:10.1016/j.jseaes.2017.06.004

Guo, H., and Zhao, J. X. (2019). The surface rupture zone and paleoseismic evidence on the seismogenic fault of the 1976 Ms 7.8 Tangshan earthquake, China. *Geomorphology* 327, 297–306. doi:10.1016/j.geomorph.2018.11.006

Guo, S. M., Li, Z. L., Cheng, S. P., Chen, X, C., and Chen, X, D., (1977). Discussion on regional structural background and the seismogenic model of the Tangshan earthquake. *Sci. Geol. Sin.* 4, 305–321. in Chinese with English abstract.

Hao, S. J., and You, H. C. (2001). A detailed detection of the Tangshan active fault using shallow seismic survey. *Seismol. Geol.* 23, 93–97. in Chinese with English abstract. doi:10.3969/j.issn.0253-4967.2001.01.012

Huang, B. S., and Yeh, Y. T. (1997). The fault ruptures of the 1976 Tangshan earthquake sequence inferred from coseismic crustal deformation. *Bull. Seismol. Soc. Am.* 87 (4), 1046–1057.

Huang, J. L., and Zhao, D. P. (2006). High-resolution mantle tomography of China and surrounding regions. *J. Geophys. Res.* 111, B09305. doi:10.1029/2005jb004066

Lai, X. L., Zhang, X. K., and Zheng, X. Y. (1998). Two-step back analysis of interfaces and velocity-3d fine structure research of Tangshan seismic region. *Acta Seismol. Sin.* 20, 590–597. in Chinese with English abstract.

Li, H. B., Pan, J. W., Sun, Z. M., Liu, D. L., Zhang, J. J., Li, C. L., et al. (2015). Seismogenic structure and surface rupture characteristics of the 2014 Ms7.3Yutian earthquake. *Acta Geol. Sin.* 89, 180–194. in Chinese with English abstract.

Li, X. R., Wang, J., Zeng, Z. X., and Dai, Q. (2017). Spatial variations of current tectonic stress field and its relationship to the structure and rheology of lithosphere around the Bohai Sea, North China. *J. Asian Earth Sci.* 139, 83–94. doi:10.1016/j.jseaes.2016.12.023

Li, Z. W., Ni, S. D., Roecker, S., Bao, F., Wei, X., Yuen, D. A., et al. (2018). Seismic imaging of source region in the 1976 Ms7.8 Tangshan earthquake sequence and its implications for the seismogenesis of intraplate earthquakes. *Bull. Seismol. Soc. Am.* 108, 1302–1313. doi:10.1785/0120170389

Lin, A. M., Guo, J. M., and Fu, B. H. (2004). Co-seismic mole track structures produced by the 2001 Ms 8.1Central Kunlun earthquake, China. *J. Struct. Geol.* 26, 1511–1519. doi:10.1016/j.jsg.2004.01.005

Lin, A. M., Rao, G., Jia, D., Wu, X., and Ren, Z. K. (2011). Co-seismic strike-slip surface rupture and displacement produced by the 2010 Mw6.9 Yushu earthquake, China, and implications for Tibetan tectonics. *J. Geodyn.* 52, 249–259. doi:10.1016/j.jog.2011.01.001

Liu, B. J., Qu, G. S., Sun, M. X., Liu, K., Zhao, C. B., Xu, X. W., et al. (2011). Crustal structures and tectonics of tangshan earthquake area: Results from deep seismic reflection profiling. *Seismol. Geol.* 33 (4), 901–912. in Chinese with English abstract.

Liu, K. (2011). *Comprehensive research on the features of strong earthquake recurrence and the coupling relationship between shallow and deep structures in the Tangshan area*. Beijing: Institute of Geology: China Earthquake Administration. in Chinese with English abstract.

Liu, K., Li, Y. F., Guo, H. W., and Zhang, Y. F. (2021). Determination of surface rupture length and analysis of Riedel shear structure of the Litang M 7.3 earthquake in west Sichuan in 1948. *Acta Geol. Sin.* 95 (8), 2346–2360. in Chinese with English abstract.

Liu, K., Qu, G. S., Chen, J. Q., Wang, W. G., and Ning, B. K. (2013). Recurrence characteristics of major earthquakes in the Tangshan area, North China. *Acta Geol. Sin. - Engl. Ed.* 87, 254–271. doi:10.1111/1755-6724.12046

Liu, Q. Y., Wang, J., Chen, J. H., Li, S. C., and Guo, B. (2007). Seismogenic tectonic environment of 1976 great tangshan earthquake: Results from dense seismic array observations. *Earth Sci. Front.* 14, 205–212. in Chinese with English abstract. doi:10.1016/s1872-5791(08)60012-3

Long, L., and Zelt, K. (1991). A local weakening of the brittle-ductile transition can explain some intraplate seismic zones. *Tectonophysics* 186, 175–192. doi:10.1016/0040-1951(91)90392-6

Mearns, E., and Sornette, D. (2021). A transfer fault complex to explain the geodynamics and faulting mechanisms of the 1976 M7.8 Tangshan earthquake China. *J. Asian Earth Sci.* 2021 (7/8), 104738. doi:10.1016/j.jseaes.2021.104738

Nabelek, J., Chen, W. P., and Ye, H. (1987). The Tangshan earthquake sequence and its implications for the evolution of the North China basin. *J. Geophys. Res.* 92, 12615. doi:10.1029/jb092ib12p12615

Qiu, Q. (1976). On the background and seismic activity of the M = 7.8 Tangshan earthquake, Hopei Province, July 28, 1976. *Acta Geophys. Sin.* 19 (4), 259–269.

Qiu, Z. H., Ma, J., and Liu, G. X. (2005). Discovery of the great fault of the Tangshan earthquake. *Seismol. Geol.* 27, 669–677. in Chinese with English abstract.

Rao, G., Lin, A. M., Yang, B., Jia, D., Wu, X., Ren, Z. K., et al. (2011). Co-seismic Riedel shear structures produced by the 2010 Mw 6.9 Yushu earthquake, central Tibetan Plateau, China. *Tectonophysics* 507, 86–94. doi:10.1016/j.tecto.2011.05.011

Shao, X. Z., Zang, J. R., Zhang, S. Y., and Chen, J. P. (1986). Investigation of deep Structures in Tangshan earthquake area. *Chin. J. Geophys.* 29, 28–41. in Chinese with English abstract.

Shedlock, K. M., Baranowski, J., Xiao, W. W., and Liang, H. X. (1987). The Tangshan aftershock sequence. *J. Geophys. Res.* 92 (B3), 2791–2803. doi:10.1029/jb092ib03p02791

Tchalenko, J., and Ambraseys, N. (1970). Structural analysis of the Dasht-eBayaz (Iran) earthquake fractures. *Geol. Soc. Am. Bull.* 81, 41. doi:10.1130/0016-7606(1970)81[41:saotdb]2.0.co;2

Tchalenko, J. (1970). Similarities between shear zones of different magnitudes. *Geol. Soc. Am. Bull.* 81, 1625. doi:10.1130/0016-7606(1970)81[1625:sbszod]2.0.co;2

Wan, T. F. (2007). *Outline of Chinese geotectonics*. Beijing: Geological Publishing House. in Chinese.

Wan, T. (1996). Length and penetration depth of Tancheng-Lujiang fault zone in eastern Asia. *Geoscience* 10 (4), 518–525. in Chinese with English abstract.

Wang, C. Y., Wang, G. M., Lin, Z. Y., Zhang, S. W., Liu, Y. S., Mao, T. E., et al. (1993). A study on fine crustal structure in Xingtai earthquake area based on deep

seismic reflection profiling. *Acta Geophys. Sin.* 36 (4), 445–452. in Chinese with English abstract.

Wang, J. M., Zheng, W. J., Chen, G. S., Yang, W. T., Chen, G. L., and Pan, Z. S. (1981). A study on the principal surface fracture belt and the cause of occurrence of the tangshan earthquake. *J. Seismol. Res.* 4, 437–450. in Chinese with English abstract.

Wang, T. M., and Li, J. P. (1984). Recurrence interval of the Tangshan earthquake. *Seismol. Geol.* 6, 77–83. in Chinese with English abstract.

Wang, Z. Q., Huang, Z. L., and Zhao, S. D. (1978). Preliminary study on ground fracture and seismic effect of the Tangshan earthquake. *Explor. Tech.* 2, 11–17. in Chinese with English abstract.

Xu, J., Niu, L. F., Wang, C. H., and Han, Z. J. (1996). Tangshan-Hejian-Cixian newly-generated seismotectonic zone. *Seismol. Geol.* 18 (3), 193–198. in Chinese with English abstract.

Xu, X. W., Yu, G. H., Wang, F., Gu, M. L., Sun, Z. G., Liu, B. J., et al. (2000). Seismogenic model for the 1966 Xingtai earthquakes- nucleation of new-born fault or strick-slip of pre-existing fault? *Earthq. Res. China* 16 (4), 364–378. in Chinese with English abstract.

Yin, A., Yu, X., Shen, Z. K., and Liu-Zeng, J. (2015). A possible seismic gap and high earthquake hazard in the North China Basin. *Geology* 43 (1), 19–22. doi:10.1130/g35986.1

You, H. C., Xu, X. W., Wu, J. P., and He, J. P. (2002). Study on the relationship between shallow and deep structures in the 1976 Tangshan earthquake area. *Seismol. Geol.* 24, 571–581. in Chinese with English abstract.

Zeng, R. S., Zhang, S. Q., Zhou, H. N., and He, Z. Q. (1985). Crustal Structure of Tangshan epicentral region and its relation to the seismogenic process of a continental earthquake. *Acta Seismol. Sin.* 7, 125–142. in Chinese with English abstract.

Zhang, X. K., Yang, Y. C., Zhao, P., Zhao, J. R., Luo, L. L., and Wang, C. L. (1994). Tree-dimensional seismic transmission seismic transmission experiment in the luanxian earthquake region north China: Tomographic determination of the upper and middle crust structure. *Chin. J. Sinica* 37, 759–768. in Chinese with English abstract.

Zhang, Z. L., Li, Q. Z., Gu, J. C., Jin, Y. M., Liu, M. Y., and Liu, W. Q. (1980). The fracture processes of the Tangshan earthquake and its mechanical analysis. *Acta Seismol. Sin.* 2, 111–129. in Chinese with English abstract.